Proceedings of the 11th Brazilian Congress of Thermal Sciences and Engineering -- ENCIT 2006
Braz. Soc. of Mechanical Sciences and Engineering -- ABCM, Curitiba, Brazil, Dec. 5-8, 2006

Paper CIT06-0688

NUMERICAL SIMULATION OF THE DISPERSION OF A CONTAMINANT SPECIE OVER OBSTACLES USING A CVFEM – FORMULATION

Clodoaldo Borges Chagas (*)
clodoaldo@dem.feis.unesp.br

Odacir Almeida Neves (**)
odacir@fem.unicamp.br

Luiz Felipe Mendes de Moura (**)
felipe@fem.unicamp.br

Rosiane Cristina de Lima
Instituto Tecnológico de Aeronáutica, Departamento de Engenharia Aeronáutica e Mecânica, Área de Aerodinâmica, Propulsão e Energia – Praça Marechal Eduardo Gomes, 50, Vila das Acácias, CEP 12228-900, São José dos Campos, São Paulo, Brasil
rosiane@ita.br

João Batista Campos Silva (*)
jbcampos@dem.feis.unesp.br

(*) Department of Mechanical Engineering, Faculty of Engineering of Ilha Solteira, Av. Brazil, 56 – P.O. Box 31
State University of São Paulo, 15385-000 – Ilha Solteira, São Paulo, Brazil
(**) Department of Thermal and Fluids Engineering, Faculty of Mechanical Engineering ,P.O. Box 6122
State University of Campinas, 13083-970 – Campinas, São Paulo, Brazil

Abstract. The main purpose of this work is the numerical computation of dispersion of a contaminant specie over a region with obstacles, using a code based in Control Volume-Finite Element Method (CVFEM). Thus, the flow, temperature and concentration fields are resolved. The turbulence treatment have been done though large eddy simulation (LES) and the sub-grid scales stresses, heat and mass fluxes have been modeled through the Smagorinsky's eddy viscosity model. The domain is discretized using nine-node finite elements and the equations are discretized into control volumes around the nodes of the finite elements. Some benchmark problems are solved to validate the numerical code and the preliminary results are presented and compared to available results from the literature.

Keywords: ***contaminant dispersion, CVFEM, large eddy simulation, incompressible flow, Smagorinsky's model***

1. Introdução

Fluid flows are of interest in several engineering practical applications as: diffusers, airfoils with separation, buildings, combustors, turbines blades and many flow-relevant systems (Driver and Seegmiller, 1985).

Most of the fluid flows are turbulent; they occur in complex domains and are governed by a non-linear partial differential equations set of the convection-diffusive type. So, practical solutions can be obtained through numerical techniques such as: The Finite Difference Method (FDM), the Finite-Volume Method (FVM) and/or the Finite Element Method (FEM). The finite volume method is the most popular method used to calculate fluid flows. However, last decades, the finite element method has been improved; enabling its usage in Computational Fluid Dynamics (CFD) and it becomes a powerful tool in the fluid flow simulations in complex geometries.

In previous works, Campos Silva & Moura (1997, 2001), Campos Silva (1998) and Campos Silva *et al.* (1999) presented a development of a control volume finite element method using a quadratic, quadrilateral nine-noded element to simulate unsteady, incompressible and viscous fluid flows. In those works no turbulence model was considered, so the results were obtained for relatively low Reynolds numbers.

The main goal of this work is twofold. Primarily, it is desired to evaluate the large eddy simulation methodology (LES) implemented in the cited code previously. A validation of the code has been done by the simulations of classical benchmark flows: lid-driven-cavity and the backward facing-step flows, (Lima, 2005). After, it is desired to simulate the dispersion of a passive pollutant by a flow of the wind, utilizing a two-dimensional geometry with blocks similar to buildings in urban areas. Some authors as: Neofytou *et al* (2006), Wong (2002), Savii (1998) investigated this kind of problem named pollutant dispersion in urban canyon.

Turbulent flows are characterized by eddies with a wide range of length and time scales. The largest eddies are typically comparable in size to the characteristic length of the mean flow. The smallest scales are responsible for the dissipation of turbulence kinetic energy. It is possible, in theory, to directly resolve the whole spectrum of turbulent scales either using an approach known as direct numerical simulation (DNS), or by the usage of turbulence models (algebraic, two-equations models, second order models) with the Reynolds Average Navier-Stokes equations (RANS), or filtering the Navier-Stokes equations by the large eddy simulation methodology. In LES, large eddies are resolved directly, while small eddies (or subgrid-scales stresses) are modeled. By the increase of the computational powerful, the use of LES to simulate fluid flows has gained many adepts. Walton *et al*. (2002) utilized the LES in a mean flow and turbulent problem in cubic street canyons, obtaining results with good agreement to experimental data.

In next sections, it will be presented the mathematical model, the numerical method and the preliminary results of the simulation of pollutant dispersion around solids like urban street canyons.

2. Mathematical model

In this section the set of equations that describe the dispersion of a passive scalar by the action of a non-isothermal flow is presented. Also, some aspects of the large-eddy simulation are presented. The filtered set of partial differential equations are:

Continuity Equation

$$\frac{\partial \bar{u}_i}{\partial x_i} = 0 \tag{1}$$

Momentum Equation

$$\frac{\partial(\rho\bar{u}_i)}{\partial t^*} + \frac{\partial(\rho\bar{u}_j\bar{u}_i)}{\partial x_j} = -\frac{\partial \bar{p}_i}{\partial x_i} + \frac{\partial}{\partial x_j}\left(\mu\frac{\partial \bar{u}_i}{\partial x_j}\right) - \frac{\partial \tau_{ij}}{\partial x_j} + \bar{S}_i \tag{2}$$

Equation of a Scalar Variable (Concentration, temperature, etc.)

$$\frac{\partial(\bar{\varphi})}{\partial t^*} + \frac{\partial(\bar{u}_j\bar{\varphi})}{\partial x_j} = \frac{\partial}{\partial x_j}\left(\Gamma^*_\varphi\frac{\partial\bar{\varphi}}{\partial x_j}\right) - \frac{\partial q_{j\varphi}}{\partial x_j} + \bar{S}_\varphi \tag{3}$$

where the properties and some variables are

ρ	density;
μ	dynamic viscosity;
$\bar{\varphi} = \bar{T}$	in temperature equation;
$\bar{\varphi} = \bar{C}$	in concentration equation;
$\Gamma^*_\varphi = k/\rho c_p$	thermal diffusivity in temperature equation;
$\Gamma^*_\varphi = D$	mass diffusivity in concentration equation;
S_i and S_φ	source terms accounting for the effects of buoyancy, heat generation (temperature equation) or chemical reaction (concentration equation);
*	dimensional variables;
- (overbar)	filtered or large scale variables.

In large-eddy simulation, the large-scale variables representing the velocity, pressure or other scalar fields are defined by a filter function in the form:

$$\bar{f}(\vec{x}) = \int_D f(\vec{x}')G(\vec{x}',\vec{x}',\Delta)d\vec{x}' \tag{4}$$

where G is a filter function, the most common filter functions are: Gaussian, Top-hat or Sharp Fourier cut-off filters, Chidambaram (1998); and Δ is the filter width, generally, $\Delta = (\Delta_x\Delta_y\Delta_z)^{1/3}$ with Δ_{x_i} being the grid size in the x_i axis.

The sub-grid-scale (sgs) stress tensor τ_{ij} appearing in Eq. (2) and the sub-grid flux $q_{j\varphi}$ in Eq. (3) come from the filtering process, they are defined as:

$$\tau_{ij} = \rho(\overline{u_i u_j} - \bar{u}_i\bar{u}_j)\,; \quad q_{j\varphi} = -\rho(\overline{u_j\varphi} - \bar{u}_j\bar{\varphi}) \tag{5}$$

which must be modeled. In this work it has been used the Smagorinsky model and the sgs stress tensor and fluxes are modeled in the form:

$$\tau_{ij} = \frac{2}{3}\rho k \delta_{ij} - 2\mu_t^* \overline{S}_{ij} \, ; \;\; q_{i\varphi} = -\Gamma_{\varphi t}^* \frac{\partial \overline{\varphi}}{\partial x_i} \tag{6}$$

where the eddy viscosity, μ_t, the turbulent kinetic energy, k and the deformation rate are defined by the following expressions:

$$\mu_t^* = \rho (C_s \Delta)^2 (2\overline{S}_{kl}\overline{S}_{kl})^{1/2} \, ; \;\; k = \frac{\tau_{ii}}{2} \, ; \;\; \overline{S}_{ij} = \frac{1}{2}\left(\frac{\partial \overline{u}_i}{\partial x_j} + \frac{\partial \overline{u}_j}{\partial x_i} \right) \tag{7}$$

The squared Smagorinsky's constant after some tests with lid-driven cavity flow was choose to be $C_s^2 = 0{,}026$, Lima (2005). The filter width was choose to be equal to the length of control volume face where the convective and diffusive fluxes are considered ($\Delta = \int_{\xi} \sqrt{(\partial x/\partial \xi)^2 + (\partial y/\partial \xi)^2}\, d\xi$ or $\Delta = \int_{\eta} \sqrt{(\partial x/\partial \eta)^2 + (\partial y/\partial \eta)^2}\, d\eta$). See Fig. 2 for reference.

After the substitution of Eq. (7) and Eq. (6) into Eq. (2) and Eq. (3) one obtains the following equations in dimensionless form:

$$\frac{\partial U_i}{\partial X_i} = 0 \tag{8}$$

$$\frac{\partial U_i}{\partial t} + \frac{\partial (U_j U_i)}{\partial X_j} = -\frac{\partial P_t}{\partial X_i} + \frac{\partial}{\partial X_j}\left(\left(\frac{1}{Re} + \nu_t \right) \frac{\partial U_i}{\partial X_j} \right) + \frac{\partial}{\partial X_j}\left(\nu_t \frac{\partial U_j}{\partial X_i} \right) + F_i \tag{9}$$

$$\frac{\partial \Phi}{\partial t} + \frac{\partial \left(U_j \Phi \right)}{\partial X_j} = \frac{\partial}{\partial X_j}\left(\left(\frac{\Gamma_\Phi}{Re} + \Gamma_{\Phi t} \right) \frac{\partial \Phi}{\partial X_j} \right) + S_\Phi \tag{10}$$

where the term of kinetic energy was included in pressure term resulting the turbulent pressure, $P_t = \overline{P} + \frac{2}{3}\frac{k}{u_0^2}$. The dimensionless variables are defined as:

$$X_i = \frac{x_i}{L} ; \;\; U_i = \frac{\overline{u}_i}{u_0} ; \;\; \overline{P} = \frac{\overline{p} - p_0}{\rho\, u_0^2} ; \;\; t = \frac{t^*}{L/u_0} ; \;\; \nu_t = \frac{\nu_t^*}{u_0 L} = \left(C_s \frac{\Delta}{L} \right)^2 \left(2\, \overline{S}_{kl}\, \overline{S}_{kl} \right)^{1/2} ; \;\; Re = \frac{\rho u_0 L}{\mu} ; \;\; Pr = \frac{\mu c_p}{k} ; \;\; Sc = \frac{\nu}{D} ,$$
$$\Phi = \frac{\left(\overline{T} - T_0 \right)}{\Delta T} \text{ or } \Phi = \frac{\overline{C}}{C_0} ; \;\; \Gamma_\Phi = \frac{1}{Pr} ; \;\; \Gamma_{\Phi t} = \frac{\nu_t}{Pr_t} \text{ or } \Gamma_\Phi = \frac{1}{Sc} ; \;\; \Gamma_{\Phi t} = \frac{\nu_t}{Sc_t} \tag{11}$$

where L is a characteristics length and variables with a subscript zero are reference variables.

3. Numerical method

The CVFEM was firstly presented by Baliga and Patankar (1980, 1983) and later by Raw and Schneider (1986). They used triangular and linear quadrilateral elements, respectively. Several authors have enhanced the CVFEM since that time till nowadays. Banaszek (1989) compared both the Galerkin and CVFEM methods in diffusion problems using six-noded and nine-noded elements. Campos Silva (1998) and Campos Silva & Moura (2001) presented the procedure of application of a nine-noded CVFEM.

The CVFEM formulation involves five basic steps: (1) discretization of the domain of interest into elements; (2) further discretization of the domain into control volumes that surround the nodes in the finite element mesh, as shown in Figure 1; (3) definition of element-based interpolation functions for variables and physical properties of the fluid; (4) derivation of algebraic equations by the usage of the sub-domain weighted residual method; and (5) assembling of the element equations forming the global matrix and choice of a procedure to solve the system of algebraic equations. In this method, each node of the finite element mesh is inside a control volume like in FVM. An element and its respective control volumes are showed in Figure 2, where are also showed the faces with convective and diffusive fluxes.

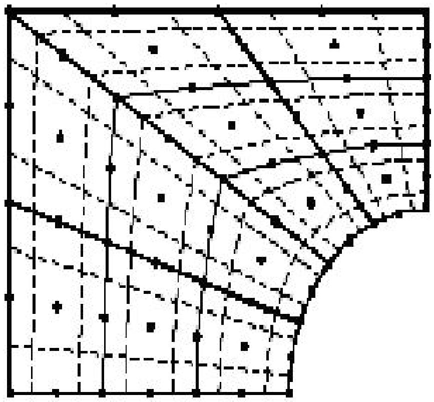

Figure 1 - Meshes of finite elements e control volumes.

Now, the integration of the Equations (8) - (10) inside each control volumes yields:

$$\int_V \frac{\partial U_i}{\partial X_i} dV = 0 \tag{12}$$

$$\int_V \frac{\partial U_i}{\partial t} dV + \oint_S \left(U_j U_i - \nu_e \frac{\partial U_i}{\partial X_j} \right) \cdot n_j dS + \int_V \frac{\partial P_t}{\partial X_i} dV = \oint_S \nu_t \frac{\partial U_j}{\partial X_i} n_j dS + \int_V F_i dV \tag{13}$$

$$\int_V \frac{\partial \Phi}{\partial t} dV + \oint_S \left(U_i \Phi - \Gamma_e \frac{\partial \Phi}{\partial X_i} \right) \cdot \overline{n}_i dS = \int_V S_\Phi dV \tag{14}$$

where S and V denoting the surface area and the volume of a control volume around a node in the element, respectively, n_j is the outward normal vector to the area of a control volume where there are convective and diffusive fluxes. The effective viscosity and diffusivity are: $\nu_e = \left(\frac{1}{Re} + \nu_t \right)$; $\Gamma_e = \frac{\Gamma_\Phi}{Re} + \Gamma_{\Phi t}$

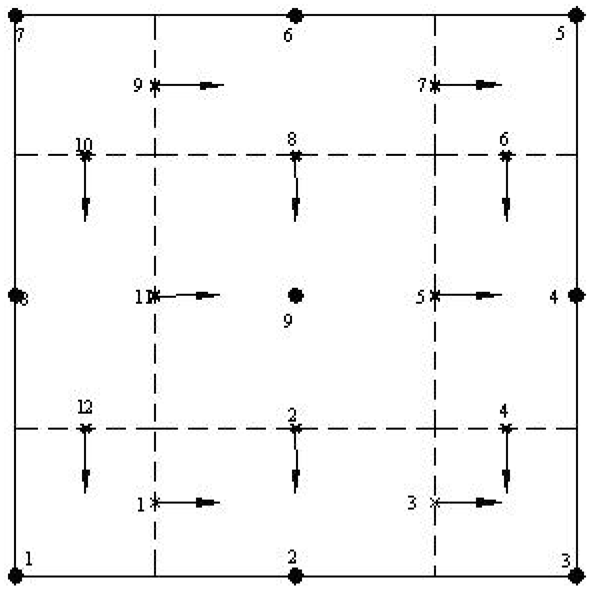

Figure 2 – Finite element divided in control volumes and integration points.

In order to transform the integrals of Eqs. (12), (13) and (14) to algebraic equations, the variables and the coordinates are interpolated like in classical Galerkin finite element method, as it's defined bellow:

$$U_i = \sum_{\alpha=1}^{nnep} N_\alpha U_{i\alpha} \tag{15}$$

$$P = \sum_{\alpha=1}^{nnel} N_\alpha P_\alpha \tag{16}$$

$$\Phi_i = \sum_{\alpha=1}^{nnep} N_\alpha \Phi_{i\alpha} \tag{17}$$

$$X_i = \sum_{\alpha=1}^{nnep} N_\alpha X_{i\alpha} \tag{18}$$

where N_α are interpolation functions of the reference element in local coordinates (Dhatt & Touzot, 1984); $U_{i\alpha}$ are the velocity components; P_α is the pressure; Φ_i is any scalar and $X_{i\alpha}$ are components of the coordinate system at nodes α of a element; nnep and nnel are nodes numbers of quadratic (parabolic) and linear elements respectively. The velocity field and scalar variables are interpolated by quadratic functions. The pressure is interpolated by linear functions (Eq.°16).

The coefficient matrices are computed element by element in local coordinates as it's showed in Fig. 3a-b and a global system of equations is assembled like in the classical finite element method. The global system of equations is solved by the frontal method proposed by Taylor & Hughes (1981). An important characteristic of this method is that the system is assembled element by element; therefore the global system never is assembled totally in memory. So, personal computers may be used for solve the cases studied.

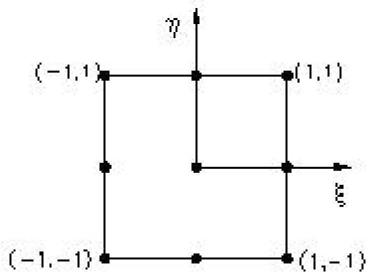

Figure 3.(a) - Element in local coordinates ξ-η

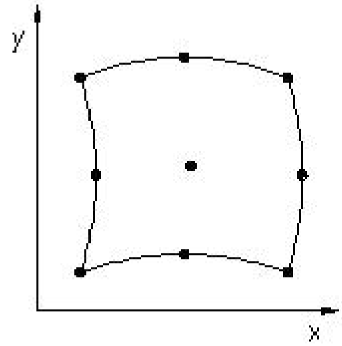

Figure 3.(b) - Element in global coordinates x-y

4. Results

The computational program was validated by Lima (2005) for classical benchmark problems: lid-driven cavity and backward-facing step flows. Dispersion of a pollutant in a cavity was also simulated by Lima with the same boundary conditions of a free convection problem with good agreement of the results with results form the literature. In that work some simulations of dispersion in urban canyons was initiated. The simulations here have been done for a flow inside a street canyon based in Savii (1998). In this case the interest is in the horizontal dispersion of pollutant specie around the obstacles.

The discretized domain for this flow is shown in Figure 4 (top view). The original dimensions of the mesh are $0 \le X \le 65$ and $0 \le Y \le 46$. The length of the buildings is 10.0; the width of upper and lower buildings is 6.0 and 2.0, respectively. The boundary conditions in the flow are $U = 1, V = 0$ and $T = 0$ at the inflow section, upper and lower boundaries; $T = 1$, in the buildings boundaries, $P = 0$ in the outlet section; C=1 between the buildings, in the center horizontal line of the domain. In this work: Re=100, Sc=0.2, Ra=0, Pr=0.7.

A qualitative comparison of the simulated concentration of this work with results from Savii (1998) is shown in Figure 5. Savii considered only transient and diffusive terms in concentration equation, while in this work the convective terms were also included. Maybe, it was the cause of differences between the results, as shown in Figure 5. In the work of Savii it was not possible to get all information about the domain of calculation and numerical values of the velocity and concentration fields.

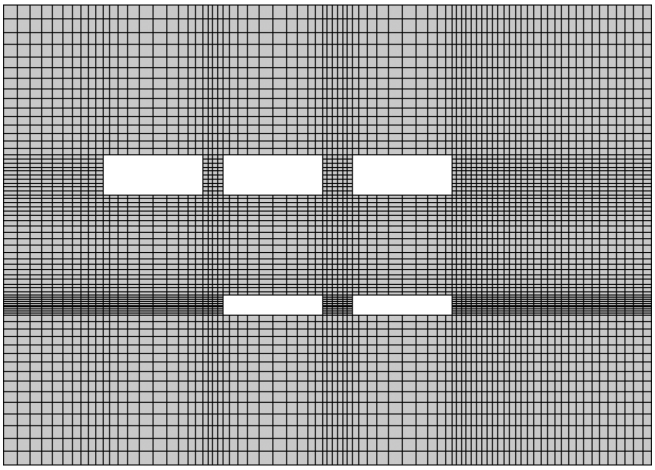

Figure 4. Discretized domain with five obstacles.

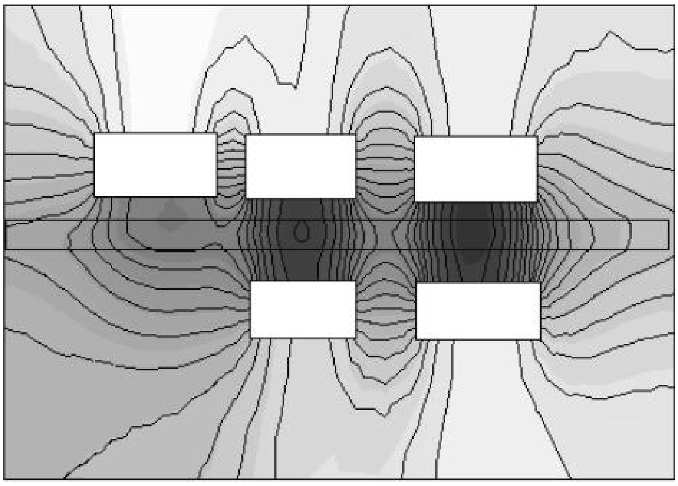

Figure 5a. Simulated concentration field, Savii (1998)

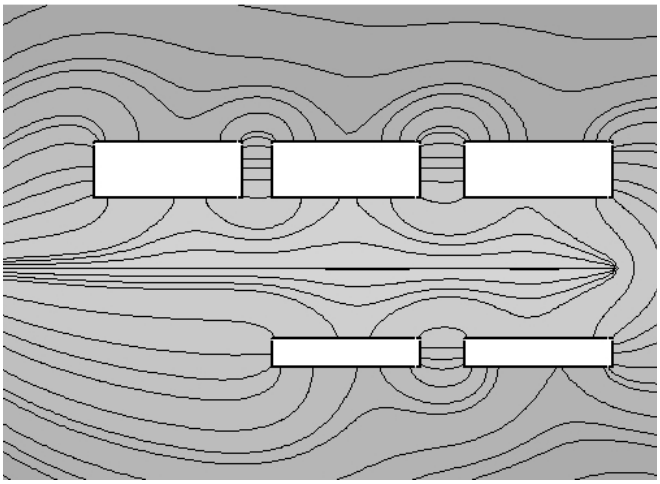

Figure 5b. Simulated concentration field, this work

The Figures 6-13 show the X-velocity profiles before the first building, between buildings and after last buildings at several time steps. Qualitatively the behavior of the velocity has been simulated; however, the size of the computational domain has to be increased. As can be seen in Figure 13 the presence of obstacles still has much influence on the outlet velocity and the length of computational domain after the obstacles seems to have been short. If the computational dimensions are appropriated, most probably the outlet velocity profile will be parabolic or more uniform. The size of the domain could be insufficient for imposed boundary conditions.

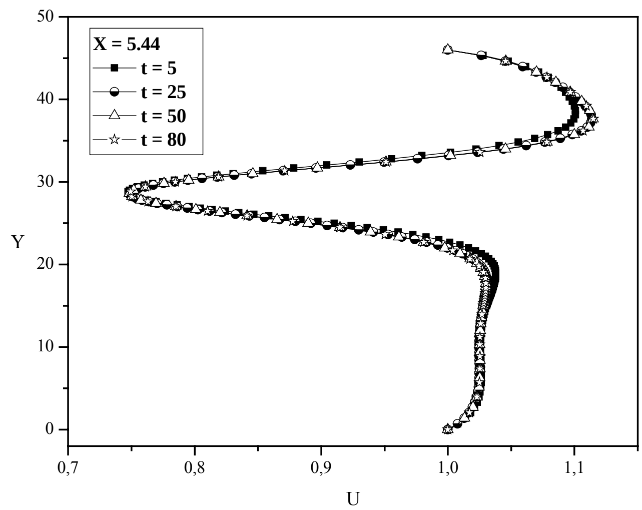

Figure 6. X-Velocity before the first building, X = 5.4.

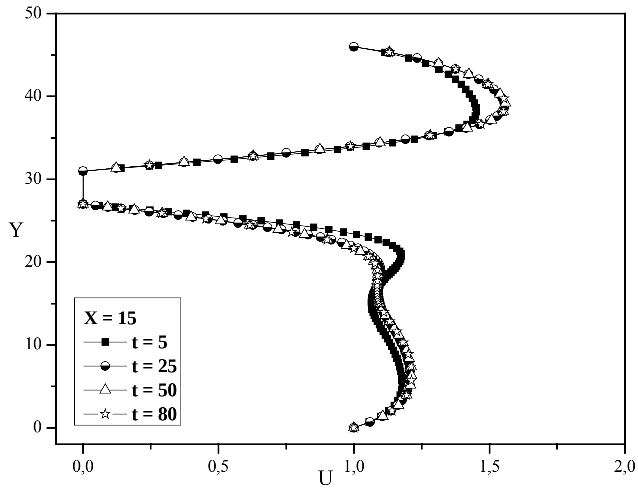

Figure 7. X-Velocity in the half of first building, X = 15.

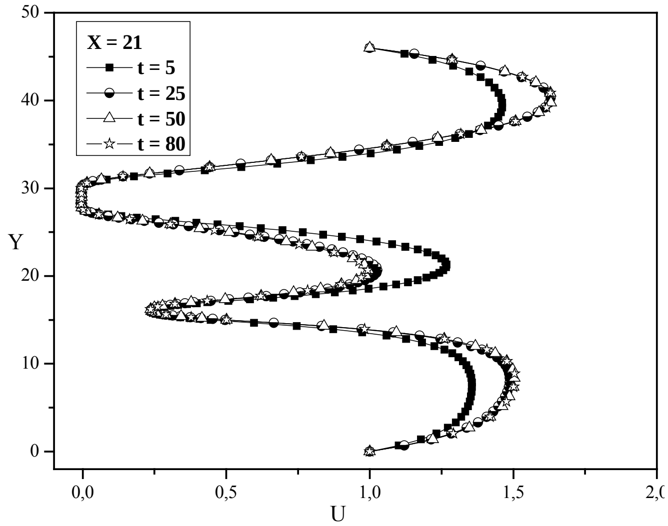

Figure 8. X-Velocity between the first and second building, X = 21.

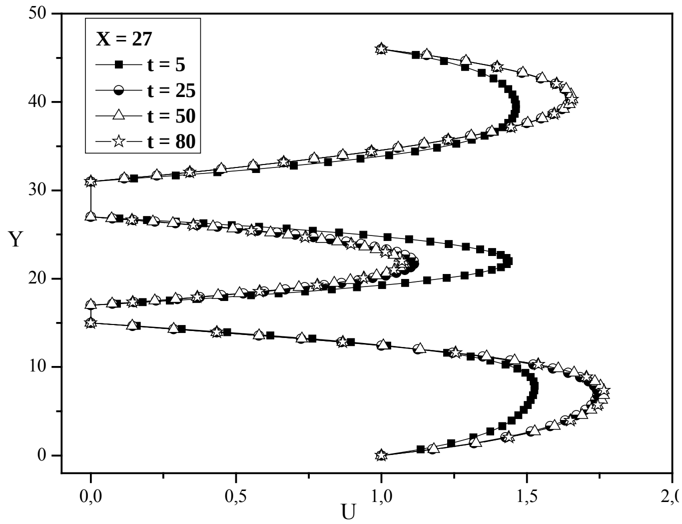

Figure 9. X-Velocity in the half of second building, X = 27.

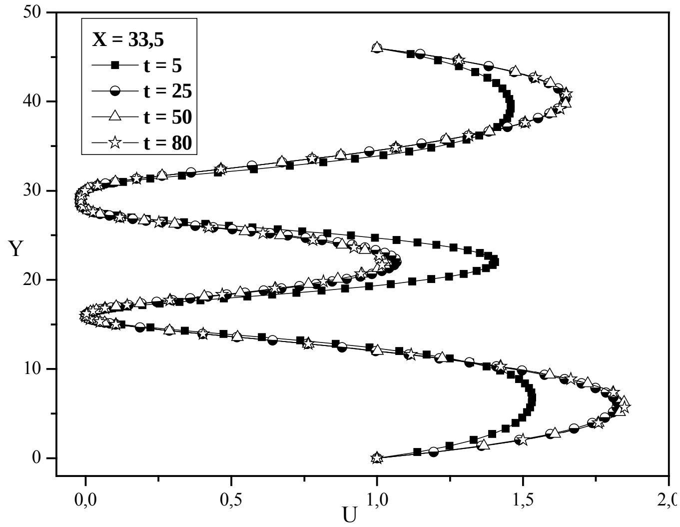

Figure 10. X-Velocity between the second and third building, X = 33.5.

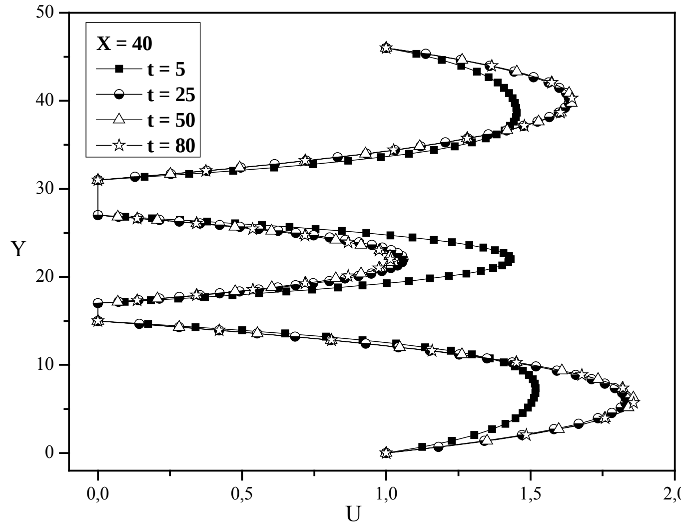

Figure 11. X-Velocity in the half of third building, X = 40.

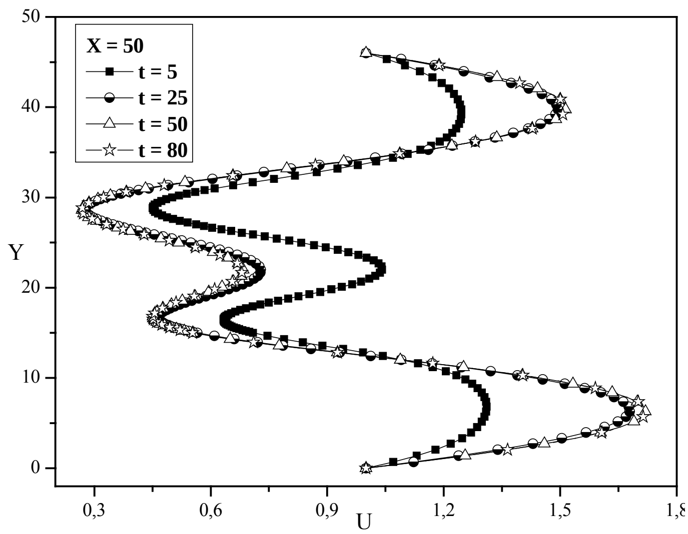

Figure 12. X-Velocity after the third building, X = 50.

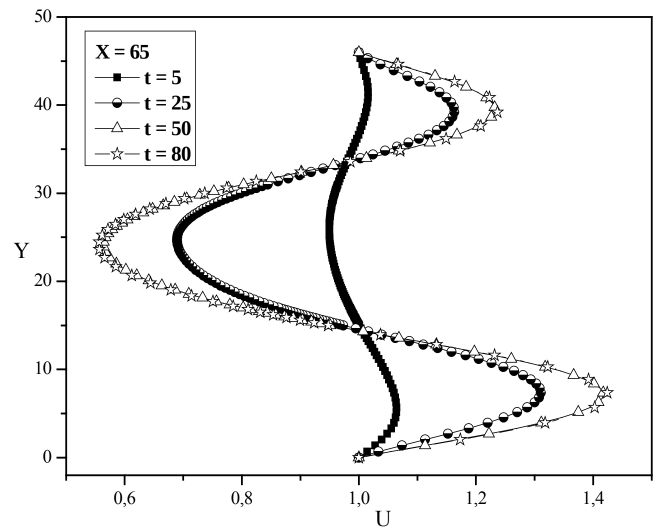

Figure 13. X-Velocity in the exit of flow, X = 65.

The evolution with time of the pollutant concentration in the domain is shown in Figures 14 to 21. Qualitatively, the results seem to be simulated with the expected behavior. It was not possible to do comparisons with experimental and other numerical results, because the authors didn't find available such results. However, the model for this type of simulation needs more investigation, mainly, for high Reynolds number flows. The stream functions and temperature field are shown in Figure 22 and 23, respectively. They seem to present the waited behavior.

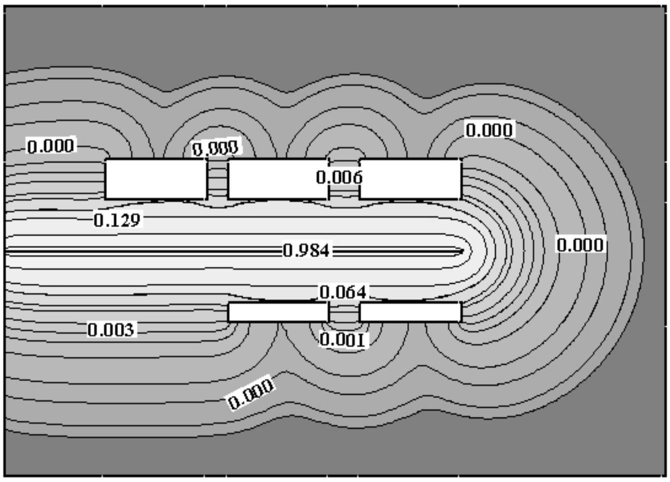

Figure 14. Pollutant concentration field at t=3

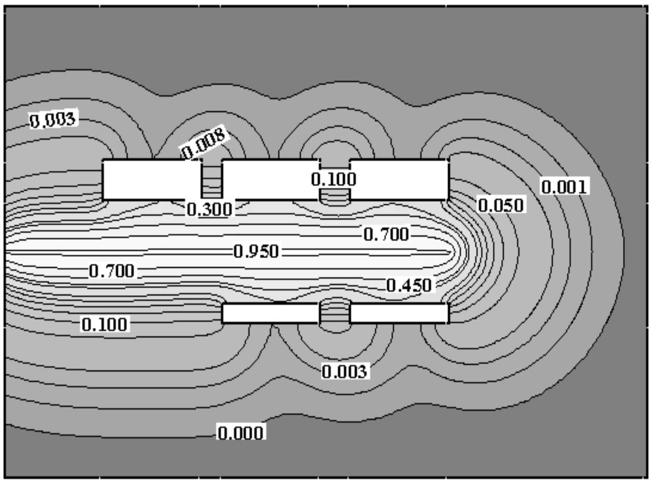

Figure 15. Pollutant concentration field at t = 12

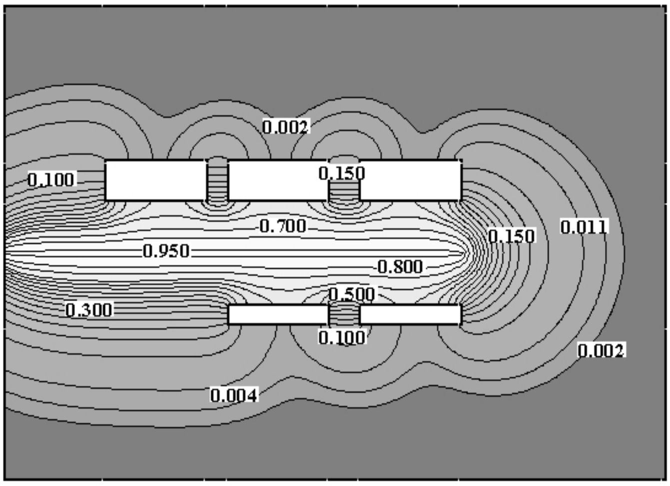

Figure 16. Pollutant concentration field at t=20

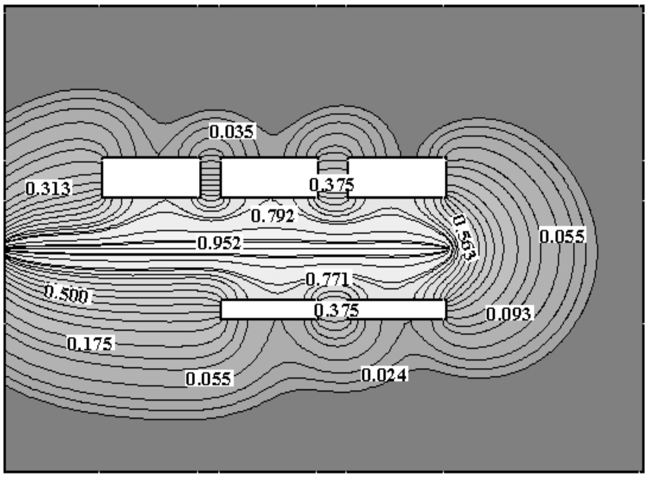

Figure 17. Pollutant concentration field at t=30

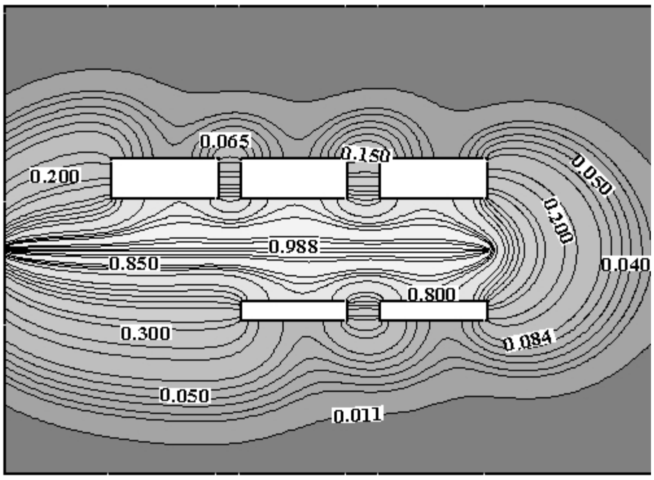

Figure 18. Pollutant concentration field at t =35

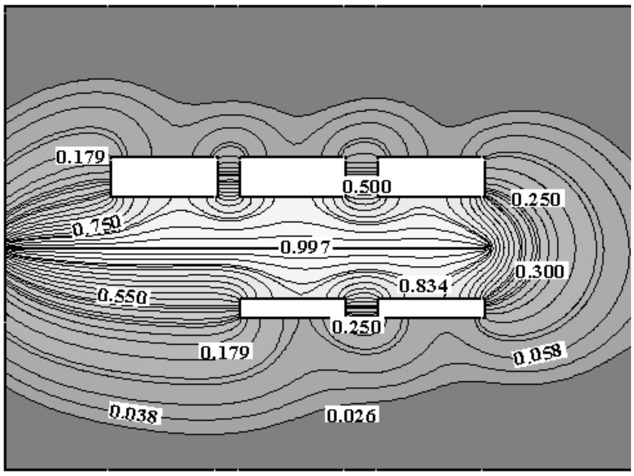

Figure 19. Pollutant concentration field at t = 40

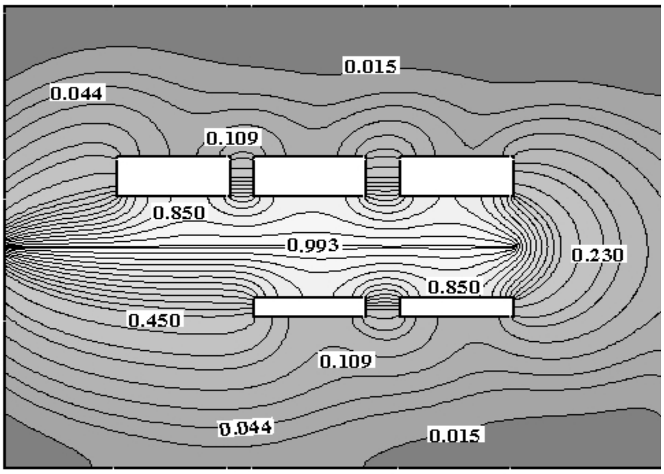

Figure 20. Pollutant concentration field at t =45

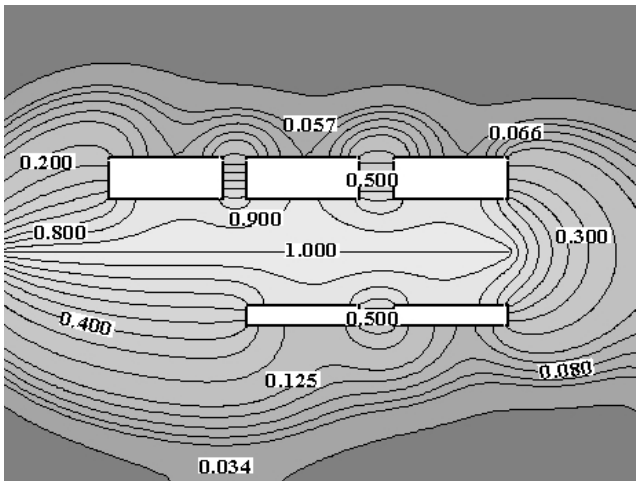

Figure 21. Pollutant concentration field at t =50

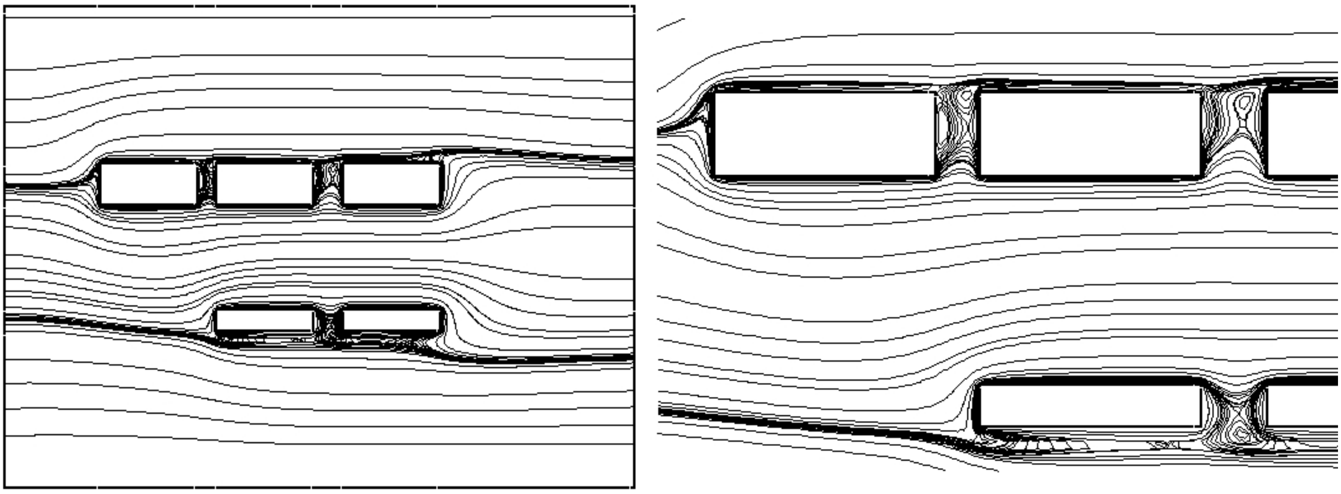

Figure 22. Stream functions

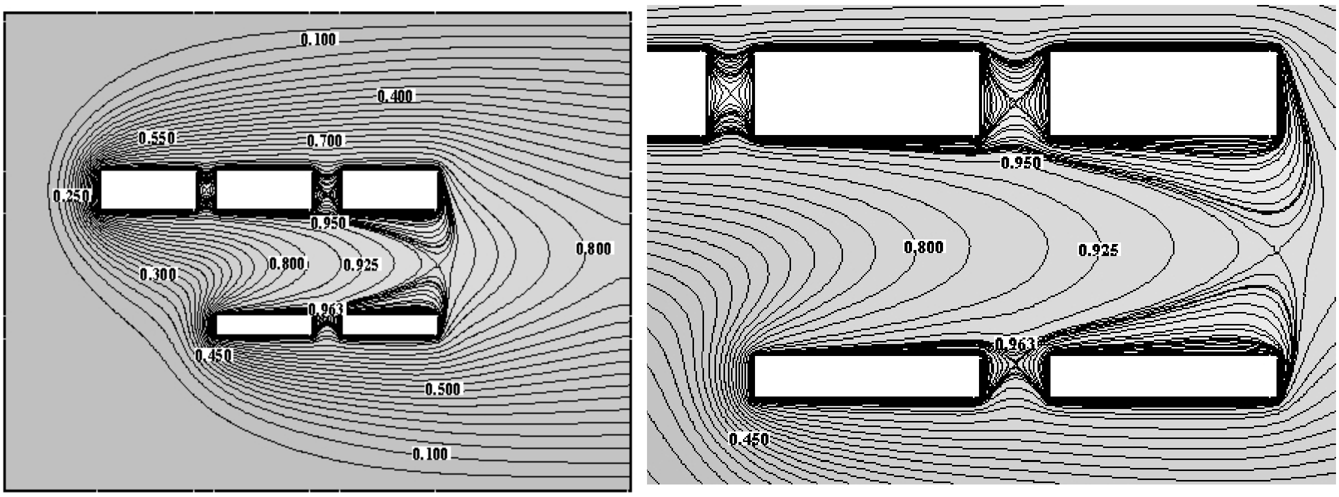

Figure 23. Temperature field

5. Conclusions

A simulation of pollutant dispersion horizontally around obstacles has been done. Qualitatively, the waited behavior of phenomenon seems have to be simulated. Some anomalous behavior of the concentration at the outflow section may be due to an insufficient size of the computational domain and a not appropriated boundary condition for velocity in the domain size considered. This has to be investigated in future works. Other arranges of obstacles, more high Reynolds number flows, effect of natural convection and different boundary conditions are subjects for the sequence of this work as well as more realistic 3D flows have to be simulated.

6. Acknowledgement

The authors would like to acknowledge the CNPq and FAPESP, process nº. 05/02301-1. The second author is CNPq – Brazil Scholarship.

7. References

Baliga, B.R. and Patankar, S.V., 1980, "A new finite-element formulation for convection-diffusion problems", Numerical Heat Transfer, Vol. 3, pp. 393-409.

Baliga, B.R. and Patankar, S.V., 1983, "A control volume finite-element method for two-dimensional fluid flow and heat transfer", Numerical Heat Transfer, Vol. 6, pp. 245-261.

Banaszek, J., 1989, "Comparison of control volume and Galerkin finite element methods for diffusion-type problems", Numerical Heat Transfer, Vol. 16, p. 59-78.

Campos Silva, J. B., and Moura, L. F. M., 2001, "A Control-Volume-Finite-Element Method (CVFEM) for Unsteady, Incompressible, Viscous Fluid Flows", Numerical Heat Transfer Part B: Fundamentals, Vol. 40 Nº 1, pp 61-82.

Campos Silva, J. B., Aparecido, J. B. & Moura, L. F. M., 1999, "A Control Volume-Finite Element Method (CVFEM) for Unsteady Fluid Flows", Anais do XV Congresso Brasileiro de Engenharia Mecânica - COBEM'99, CD ROM, Águas de Lindóia/SP.

Campos Silva, J.B. and Moura, L.F.M., 1997, "Numerical simulation of fluid flow by the control volume-finite element method", Proceedings (in CD-ROM) of the XIV Brazilian Congress of Mechanical Engineering - COBEM97, December 8-12, Bauru-SP, Brazil, paper code 041, 8p.

Campos Silva, J.B., 1998, "Numerical simulation of fluid flow by the finite element method based on control volumes", Doctorate Thesis (in Portuguese), State University of Campinas, Campinas, São Paulo, Brazil.

Chidambaram, N., 1998, "Colocated-grid Finite Volume Formulation for the Large Eddy Simulation of Incompressible and Compressible Turbulent Flows", Graduate College, Department of Mechanical Engineering, Iowa State University, Ames, Iowa, USA. M.Sc. Thesis.

Dhatt, G. and Touzot, G., 1984, "Une Presentation de la Méthode des Éléments Finis", Deuxieme Édition, Maloine S.A. Éditeur, Paris.

Driver, D. M. and Seegmiller, H. L., 1985, "Features of a reattaching turbulent shear layer in divergent channel flow". AIAA Journal, Vol. 23, nº 2, pp. 163-173.

Lima, R.C., 2005, "Simulação de Grandes Escalas de Escoamento Incompressíveis com Transferência de Calor e Massa por um Método de Elementos Finitos de Subdomínio", Dissertação de Mestrado, Universidade Estadual Paulista "Júlio de Mesquita Filho", Faculdade de Engenharia, Ilha Solteira, São Paulo, Brasil.

Neofytou, P., Venetsanos, A.G., Rafailidis, S., Bartzis, J.G., 2006, "Numerical investigation of the pollution dispersion in an urban street canyon", Environmental Modelling & Software 21, pp. 525–531.

Raw, M.J. and Schneider, G.E., 1986, "A skewed, positive influence coefficient up-winding procedure for control-volume-based finite-element convection-diffusion computation", Numerical Heat Transfer, Vol. 9, pp. 1-26.

Savii, G.G., 1998, "Simulation of Air Pollution in Urban Area using Finite Element Methods", Proceedings of 3rd International Conference on Technical Informatics – CONTI'98, Timisoara, Romania, October, 1998. Sci.Bull."Politehnica" Univ. Timisoara, Trans. Comp. Autom., Vol.43 (57), 1998, pp.96-99.

Taylor, C., and Hughes, T.G., 1981, "Finite Element Programming of the Navier-Stokes Equations", Pineridge Press Ltd, Swansea, U.K.

Walton, A., Cheng, A.Y.S., Yeung, W.C., 2002, "Large-eddy simulation of pollution dispersion in an urban street canyon – Part I: comparison with field data". Atmospheric Environment 36, pp. 3601–3613.

Wong, A.Y.T., Chan, A.T. and So, E.S.P., 2002, "Computational Analysis of Wind Flow and Pollutant Dispersion in an Urban Street Canyon", The 15th Engineering Mechanics Division Conference of the American Society of Civil Engineers at Columbia University in the City of New York, New York, NY June 2-5.